Acoustic Response of a Multilayer Panel with Viscoelastic Material

M. Abid and M. S. Abbes
University of Sfax, Enis, Tunisia

J. D. Chazot
University of Technology of Compiegne, UTC, France

L. Hammemi
University of Sfax, Enis, Tunisia

M. A. Hamdi
University of Technology of Compiegne, UTC, France

M. Haddar
University of Sfax, Enis, Tunisia

(Received August 19, 2010, Provisionally Accepted November 15, 2011, Accepted February 1, 2012)

The development of materials both rigid and light with high damping effect and acoustic insulation is possible by using a multilayer panel with viscoelastic material. The rigidity of a multilayer panel is provided by its elastic layers, and damping is provided by viscoelastic layers. Prediction of the behavior of such systems in the conception phase is very important to determine the most important parameters in a multilayer panel in the aim to maximize insulation and to properly design this panel for several applications. In this work we have developed a model based on transfer matrix method, which is an analytic method to predict behavior of infinite layer subjected to a plane wave with an oblique incidence.

Notation

v_1	Velocity in the $\boldsymbol{x}_1$ direction
v_3	Velocity in the $\boldsymbol{x}_3$ direction
G	Shear modulus
$\boldsymbol{\nu}$	Poisson's ratio
$\boldsymbol{\rho}$	Mass density
$\boldsymbol{\omega}$	Angular frequency
$\boldsymbol{k_{comp}}$	Wave number of compressional wave
k_{cis}	Wave number of shear wave
ϕ	Compressional wave potential
ψ	Shear wave potential
k_1	Wave number in the x_1 direction
$k_{\phi 3}$	Wave number of the compressional wave in the x_3 direction
$k_{\psi 3}$	Wave number of the shear wave in the x_3 direction
σ_{33}	Normal stress
σ_{31}	Shear stress
p	Pression of the fluid
$\mathbf{V}$	State vector
$\mathbf{I_{f,s}}$, $\mathbf{J_{f,s}}$	Interface matrix
$\mathbf{I_{s,f}}$, $\mathbf{J_{s,f}}$	Interface matrix
$\mathbf{T}$	Transfer matrix
Z_c	Characteristic impedance of the fluid
Z_a	Impedance at the left-hand side of the material
Z_a	Impedance at the left-hand side of the material
T	Transmission coefficient
R	Reflection coefficient
TL	Transmission loss
τ	Acoustic transparency
E^*	Complex Youngs modulus
τ, τ_u	Relaxation time of the viscoelastic material
E_∞	Modulus in high frequency
E_0	Modulus at low frequency
f_{carac}	Characteristic frequency
δ	Phase angle for the viscoelastic material
f_{coin}	Coincidence frequency
D	Flexural rigidity

1. INTRODUCTION

Multilayer panels are widely used as sound insulation in automotive industries and building acoustics. Studies of acoustic response and wave propagation through stratified material are of paramount importance for the optimum design of a multilayer panel that is both rigid and light. In order to increase acoustic insulation properties of multilayered panels, many configurations including plates, impervious screens, and layers of air and viscoelastic media have been studied. The behavior of these combinations of materials depends more or less on the dimensions and the boundary conditions at the edges. Nevertheless, interesting results can be obtained by modelling the samples as infinite plates subjected to incident plane waves. Using the transfer matrix related to each layer considerably

simplifies the modeling and offers other advantages like the wide frequency range applicability of the method. Moreover using the transfer matrix takes into account dominant physical phenomena like the mass law. This method, however, cannot take into account the boundary condition and cannot predict the response of a deterministic excitation. The Transfer Matrix Method (TMM) was developed first by Thomson[1] and used by many authors.[2–6] Lee and Xu developed a modified transfer matrix method for prediction of transmission loss of multilayer acoustic materials.[7] The transfer matrix is modified with plate theory for multilayer prediction. Another improvement of the transfer matrix method was done by Villot and Guigou to take into account the boundary effect, which is notable in low frequency.[8] Villot and Goigou apply a spatial windowing function depending on the plate dimension, to overcome the problem.

The TMM consists in writing the displacements and stresses in terms of wave potential functions to predict the response of the multilayer panel subjected to a given pressure. The transition from one layer to another of the same nature is done by multiplying the transfer matrix of each layer. If the layers are of different nature, we use interface matrices.[9] The transfer matrix method is best suited for the analysis of multilayer panels and passive acoustical filters, and it is well adapted to computers.[5]

The main objective of this research is to develop an easy and rapid method allowing one to predict the acoustic parameters of viscoelastic materials to improve the acoustic insulation of multilayer panels. In this study, a model based on TMM approach associated with fractional calculus for the viscoelastic material is developed.

This paper is divided into three parts. First, we describe the TMM to predict the Transmission Loss Factor of a multilayer panel, denoted TL and defined over a given frequency range. In the second part, we present a model for the viscoelastic layer based on fractional calculus.[10] In the last section, a parametric study is established by combining the viscoelastic models with transfer matrix method.

2. PROPAGATION THROUGH A STRATIFIED MATERIAL

2.1. Determination of the Transfer Matrix

Figure 1 shows a random stratified material made up of n layers and placed in an ambient fluid. Each layer i can be fluid, solid, or viscoelastic material and can have a constant thickness. The lateral dimensions of the layers are assumed to be infinite. The first layer is submitted to an incident plane acoustical wave, and the transmitted waves are evaluated on the final layer. The surrounding fluid is considered to be semi-infinite on both sides of the multilayer panel. The incident wave makes an angle θ with the x_3 axis. The global transfer matrix [**T**] of the stratified material is the product of all elementary transfer matrices [$\mathbf{T_i}$] of each layer.

For a single layer, it is assumed that the velocity field $v(x_1, x_3)$ can be separated into an irrotational and a divergence-free part as follows:[5]

$$\boldsymbol{v} = \mathbf{grad}\phi + rot\psi = v_1\boldsymbol{x}_1 + v_3\boldsymbol{x}_3. \tag{1}$$

One can write

$$v_1 = \frac{\partial\phi}{\partial x_1} + \frac{\partial\psi}{\partial x_3}; \tag{2}$$

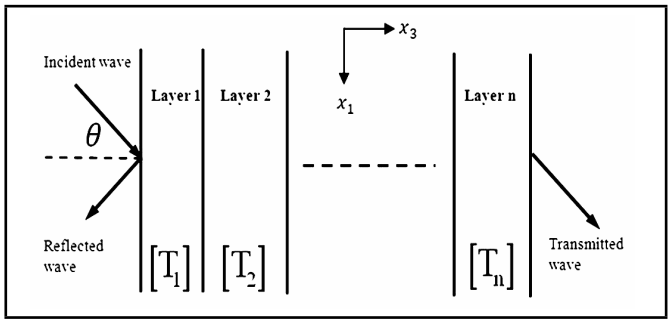

Figure 1. Multilayered panel.

$$v_3 = \frac{\partial\phi}{\partial x_3} - \frac{\partial\psi}{\partial x_1}. \tag{3}$$

Equations of motion can be written in term of velocity:[11]

$$G\left\{\Delta\boldsymbol{v} + \frac{1}{1-2\nu}\mathrm{grad.div}\,(\boldsymbol{v})\right\} = \rho\frac{\partial^2\boldsymbol{v}}{\partial t^2}; \tag{4}$$

where Δ is the Laplacian operator, ρ is the mass density, and G is the shear modulus. It can be shown that ϕ and ψ satisfy the wave equations:

$$G\frac{2\,(1-\nu)}{(1-2\nu)}\left(\frac{\partial^2}{\partial x_1^2} + \frac{\partial^2}{\partial x_3^2}\right)\phi = \rho\frac{\partial^2\phi}{\partial t^2}; \tag{5}$$

$$G\left(\frac{\partial^2}{\partial x_1^2} + \frac{\partial^2}{\partial x_3^2}\right)\psi = \rho\frac{\partial^2\psi}{\partial t^2}. \tag{6}$$

With the time dependence of all state variables being $\mathrm{e}^{j\omega t}$, ϕ and ψ satisfy

$$\left(\frac{\partial^2}{\partial x_1^2} + \frac{\partial^2}{\partial x_3^2}\right)\phi + k_{comp}^2\phi = 0; \tag{7}$$

$$\left(\frac{\partial^2}{\partial x_1^2} + \frac{\partial^2}{\partial x_3^2}\right)\psi + k_{cis}^2\psi = 0; \tag{8}$$

where

$$k_{comp}^2 = \frac{\omega^2\rho}{\mathrm{G}}\frac{1-2\nu}{2-2\nu} = \left(\frac{\omega}{c_{comp}}\right)^2; \tag{9}$$

$$k_{cis}^2 = \frac{\omega^2\rho}{\mathrm{G}} = \left(\frac{\omega}{c_{cis}}\right)^2. \tag{10}$$

The notation k_{comp} and k_{cis} represent the waves number respectively of compressional and shear waves. The symbols ϕ and ψ are respectively the compressional wave potential and shear wave potential.

These potentials can be written as

$$\phi = A_1 e^{j(\omega t - k_{\phi 3}x_3 - k_1x_1)} + A_1' e^{j(\omega t + k_{\phi 3}x_3 - k_1x_1)}; \tag{11}$$

$$\psi = A_2 e^{j(\omega t - k_{\psi 3}x_3 - k_1x_1)} + A_2' e^{j(\omega t + k_{\psi 3}x_3 - k_1x_1)}. \tag{12}$$

Here k_1 is the wave number in the x_1 direction; $k_{\phi 3}$ is the wave number of the compressional wave in the x_3 direction; $k_{\psi 3}$ is the wave number of the shear wave in the x_3 direction; and k_1, $k_{\phi 3}$, $k_{\psi 3}$, k_{comp}, and k_{cis} are related with the following equations:

$$k_{\phi 3} = \left(k_{comp}^2 - k_1^2\right)^{1/2}; \tag{13}$$

$$k_{\psi 3} = \left(k_{cis}^2 - k_1^2\right)^{1/2}. \tag{14}$$

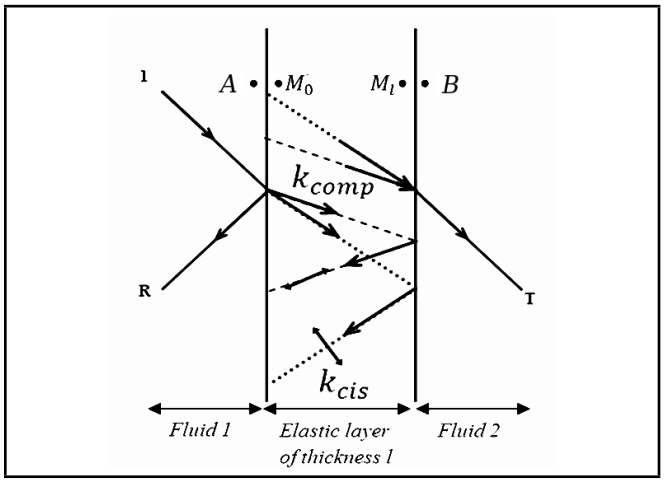

Figure 2. Waves in elastic media.

Figure 2 shows a schematic decomposition of an incident wave into compressional and shear waves. The pressure amplitude of the incident wave is taken equal to unity to simplify the notation, so that the amplitude of the transmitted and reflected waves, T and R, are respectively equal to the transmission and reflection coefficient.

For a two-dimensional case, the normal stress σ_{33} and shear stress σ_{31} are, respectively, given by the classical equations:[11]

$$\sigma_{33} = \frac{2\mathrm{G}}{\mathrm{j}\omega}\left\{\frac{\partial v_3}{\partial x_3} + \frac{\nu}{1-2\nu}\left(\frac{\partial v_1}{\partial x_1} + \frac{\partial v_3}{\partial x_3}\right)\right\}; \text{ and} \quad (15)$$

$$\sigma_{31} = \frac{\mathrm{G}}{\mathrm{j}\omega}\left(\frac{\partial v_1}{\partial x_3} + \frac{\partial v_3}{\partial x_1}\right). \quad (16)$$

After inserting Eqs. (11) and (12) into Eqs. (2), (3), (15), and (16), the state vector $\mathbf{V}(M)$, defined at a point M in the layer, can be written as follows:

$$\mathbf{V}(M) = \mathbf{V}(x_3) = [v_1\ v_3\ \sigma_{33}\ \sigma_{31}]^T; \quad (17)$$

$$\mathbf{V}(M) = \mathbf{\Gamma}(x_3)\,\mathbf{A}; \quad (18)$$

with

$$\mathbf{A} = \left[A_1 + A_1^{'} \quad A_1 - A_1^{'} \quad A_2 + A_2^{'} \quad A_2 - A_2^{'}\right]^T; \quad (19)$$

$$\mathbf{\Gamma}(x_3) = \left[\begin{array}{cc} -\mathrm{j}k_1\cos(k_{\phi 3}x_3) & -k_1\sin(k_{\phi 3}x_3) \\ -k_{\phi 3}\sin(k_{\phi 3}x_3) & -jk_{\phi 3}\cos(k_{\phi 3}x_3) \\ -\frac{2\mathrm{G}\cos(k_{\phi 3}x_3)}{\mathrm{j}\omega}KK & \frac{2\mathrm{G}\sin(k_{\phi 3}x_3)}{\mathrm{j}\omega}KK \\ \frac{2\mathrm{G}}{\omega}k_1k_{\phi 3}\sin(k_{\phi 3}x_3) & \mathrm{j}\frac{2\mathrm{G}}{\omega}k_1k_{\phi 3}\cos(k_{\phi 3}x_3) \end{array}\right.$$
$$\left.\begin{array}{cc} -k_{\psi 3}\sin(k_{\psi 3}x_3) & -\mathrm{j}k_{\psi 3}\cos(k_{\psi 3}x_3) \\ \mathrm{j}k_1\cos(k_{\psi 3}x_3) & k_1\sin(k_{\psi 3}x_3) \\ -\frac{2\mathrm{G}}{\omega}k_1k_{\psi 3}\sin(k_{\psi 3}x_3) & -j\frac{2\mathrm{G}}{\omega}k_1k_{\psi 3}\cos(k_{\psi 3}x_3) \\ -\mathrm{j}\frac{\mathrm{G}}{\omega}\cos(k_{\psi 3}x_3)\left(k_1^2 - k_{\psi 3}^2\right) & -\frac{\mathrm{G}}{\omega}\sin(k_{\psi 3}x_3)\left(k_1^2 - k_{\psi 3}^2\right) \end{array}\right]; \quad (20)$$

$$KK = \left(k_{\phi 3}^2 + \frac{\nu}{1-2\nu}\left(k_1^2 + k_{\phi 3}^2\right)\right). \quad (21)$$

We consider two points M_0 and M_l respectively on both sides of the layer. One can write

$$\mathbf{V}(M_0) = [\mathbf{T}]\,\mathbf{V}(M_l). \quad (22)$$

Thus, using Eq. (18) at M_0 and M_l, the transfer matrix of a single layer is expressed as

$$[\mathbf{T}] = \mathbf{\Gamma}(0)\,\mathbf{\Gamma}(l)^{-1}. \quad (23)$$

2.2. Equation of Coupled System

In fact, the single-layer plate is in contact with fluid 1 on the left and fluid 2 on the right (Fig. 2). To describe properly the coupled system, equations of continuity are necessary. Let A and B be two points, close to the elastic layer, respectively situated on the left infinite acoustic field and on the right one. Referring to Allard et al.,[9] one can write:

$$\sigma_{33}(M_0) = -p(A); \quad (24)$$

$$\sigma_{31}(M_0) = 0; \quad (25)$$

$$v_3(M_0) = v_3(A). \quad (26)$$

Equations of continuity are considered between M_l and B; the equation of the coupled system can be written as

$$[\mathbf{I_{f,s}}]\,\mathbf{V}(A) + [\mathbf{J_{f,s}}]\,\mathbf{V}(M_0) = 0; \quad (27)$$

$$[\mathbf{I_{s,f}}]\,\mathbf{V}(M_l) + [\mathbf{J_{s,f}}]\,\mathbf{V}(B) = 0; \quad (28)$$

with

$$\mathbf{V}(A) = \left[\begin{array}{cc} p(A) & v_3(A) \end{array}\right]^T; \quad (29)$$

$$\mathbf{V}(B) = \left[\begin{array}{cc} p(B) & v_3(B) \end{array}\right]^T. \quad (30)$$

The symbols $[\mathbf{I_{f,s}}]$ and $[\mathbf{J_{f,s}}]$ represent interface matrices between fluid and solid; the symbols $[\mathbf{I_{s,f}}]$ and $[\mathbf{J_{s,f}}]$ represent interface matrices between solid and fluid. These matrices are equal to:

$$[\mathbf{I_{f,s}}] = \left[\begin{array}{cc} 0 & -1 \\ 1 & 0 \\ 0 & 0 \end{array}\right]; \quad (31)$$

$$[\mathbf{J_{f,s}}] = \left[\begin{array}{cccc} 0 & 1 & 0 & 0 \\ 0 & 0 & 1 & 0 \\ 0 & 0 & 0 & 1 \end{array}\right]; \quad (32)$$

$$[\mathbf{I_{s,f}}] = [\mathbf{J_{f,s}}]; \quad (33)$$

$$[\mathbf{J_{s,f}}] = [\mathbf{I_{f,s}}]. \quad (34)$$

When inserting Eq. (22) into Eq. (27), the equation of the coupled system of (27) and (28) can be written as

$$[\mathbf{D}]\,\mathbf{V_D} = 0; \quad (35)$$

with $[\mathbf{D}] = \left[\begin{array}{ccc} [\mathbf{I_{f,s}}] & [\mathbf{J_{f,s}}]\,[\mathbf{T}] & 0 \\ 0 & [\mathbf{I_{s,f}}] & [\mathbf{J_{s,f}}] \end{array}\right]$ and $\mathbf{V_D} = \left[\begin{array}{ccc} \mathbf{V}(A) & \mathbf{V}(M_l) & \mathbf{V}(B) \end{array}\right]^T$.

2.3. Reflection and Transmission Coefficients

Acoustic propagation in the single layer panel of Fig. 2 is completely defined by Eq. (35), but more information is necessary to define the acoustic field. For example, since the layer of air on the right-hand side of the panel is semi-infinite, the impedance at B is given by

$$Z_b = \frac{p(B)}{V_3(B)} = \frac{Z_c}{\cos\theta}; \quad (36)$$

where Z_c is the characteristic impedance of the medium. In the case of air medium we have $Z_c = \rho_{\mathrm{air}}\mathrm{c}_{\mathrm{air}}$. Equation system (35) becomes

$$\left[\mathbf{D}^{'}\right] = \left[\begin{array}{cccc} & & [\mathbf{D}] & \\ 0 & \ldots & 0-1 & Z_b \end{array}\right]. \quad (37)$$

The impedance Z_a of the incident field at the left-hand side of the panel (Fig. 2) can be calculated by adding to the Eq. (37) the next one:

$$Z_a = \frac{p(A)}{V_3(A)}. \tag{38}$$

Thus, Eq. (37) becomes

$$[\mathbf{D}''] = \begin{bmatrix} -1 & Z_a & \dots & 0 \\ & & [\mathbf{D}] & \\ 0 & & \dots & -1 \quad Z_b \end{bmatrix}. \tag{39}$$

For a nontrivial solution of Eq. (37), the determinant of matrix $[\mathbf{D}'']$ must be equal to zero. This allows us to write

$$Z_a = -\frac{\left|\mathbf{D}_1'\right|}{\left|\mathbf{D}_2'\right|}; \tag{40}$$

where $|\mathbf{D}_1'|$ is the determinant of the matrix $\mathbf{D}'$ without its first column, and $|\mathbf{D}_2'|$ is the determinant of the matrix $\mathbf{D}'$ without its second column. Now we can calculate the reflection coefficient R with the following expression

$$R = \frac{Z_a - Z_b}{Z_a + Z_b}. \tag{41}$$

To predict the transmission coefficient T we add to Eq. (37) the following one:

$$\frac{p(A)}{p(B)} = \frac{1+R}{T}. \tag{42}$$

We obtain

$$[\mathbf{D}'''] = \begin{bmatrix} \frac{T}{1+R} & 0 & \dots & 0 & -1 & 0 \\ & & [\mathbf{D}] & & & \\ 0 & 0 & \dots & 0 & -1 & Z_b \end{bmatrix}. \tag{43}$$

For a non trivial solution of Eq. (43), the determinant of matrix $[\mathbf{D}''']$ must be equal zero, and this allows us to write:

$$T = (1+R)\frac{|\mathbf{D}_7'|}{|\mathbf{D}_1'|}. \tag{44}$$

2.4. Transmission Loss

The transmission loss TL is given by

$$\mathrm{TL} = 10\log_{10}\left(\frac{1}{\tau}\right); \tag{45}$$

where τ is the acoustic transparency defined as follows:

$$\tau = \frac{\mathcal{P}_T}{\mathcal{P}_I}. \tag{46}$$

The symbols $\mathcal{P}_T$, $\mathcal{P}_I$ represent respectively the transmitted and the incident power waves, and finally

$$\mathrm{TL} = 10\log_{10}\frac{\mathcal{P}_I}{\mathcal{P}_T} = 10\log_{10}\left(\frac{p_i^2/2Z_{fluid1}}{p_t^2/2Z_{fluid2}}\right); \tag{47}$$

where p_i, p_t represent respectively the amplitude of the incident and the transmitted waves. In this case $p_i = 1$ and $p_t = T$, hence

$$\mathrm{TL} = -20\log_{10}(T). \tag{48}$$

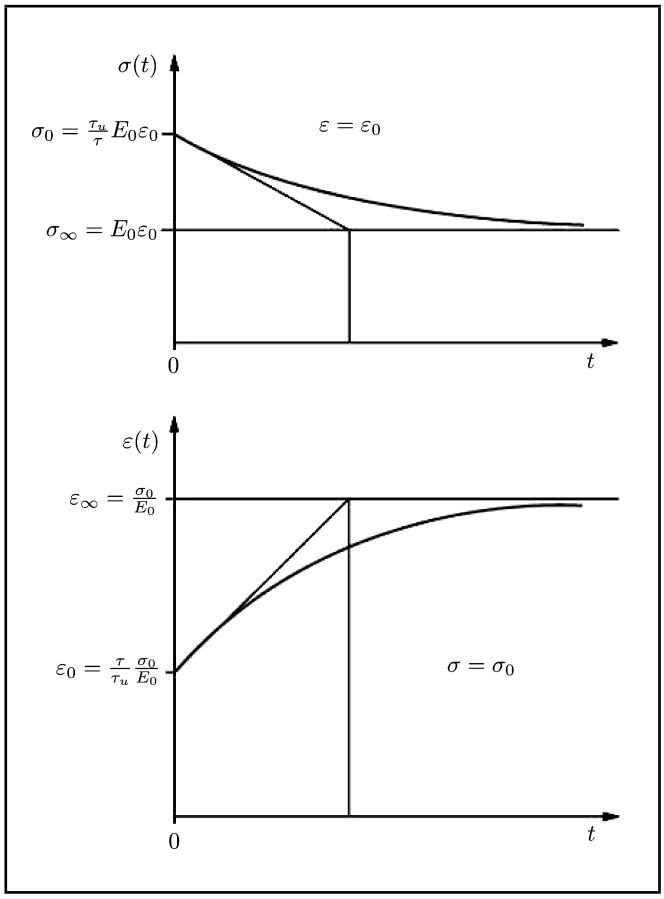

Figure 3. Relaxation and creep experience of a standard viscoelastic material.[12]

3. VISCOELASTIC MODEL

Mechanical characteristics of viscoelastic material depend on excitation frequency. To describe such material, we use a complex representation of the Young modulus[10]:

$$E^*(\mathrm{j}\omega) = E_0\frac{1+\mathrm{j}\omega\tau_u}{1+\mathrm{j}\omega\tau}; \tag{49}$$

$$E^*(\mathrm{j}\omega) = E' + \mathrm{j}E''; \tag{50}$$

with

$$E' = E_0\frac{1+\tau\tau_u\omega^2}{1+\omega^2\tau^2}; \tag{51}$$

$$E'' = E_0\frac{\omega(\tau_u - \tau)}{1+\omega^2\tau^2}. \tag{52}$$

Here E' and E'' are respectively the real and imaginary parts of the complex modulus E^*, τ and τ_u are relaxation times of the viscoelastic material determined experimentally with relaxation and creep experiences.[12]

In the relaxation experience, the strain is constantly held, and the stress decreases over time. In addition, in the creep experience, the stress is constantly held and the strain increases over time.

Stress and strain are out of phase, the phase angle is defined as the ratio between the imaginary and real part of the complex modulus:

$$\tan\delta = \frac{E''}{E'}. \tag{53}$$

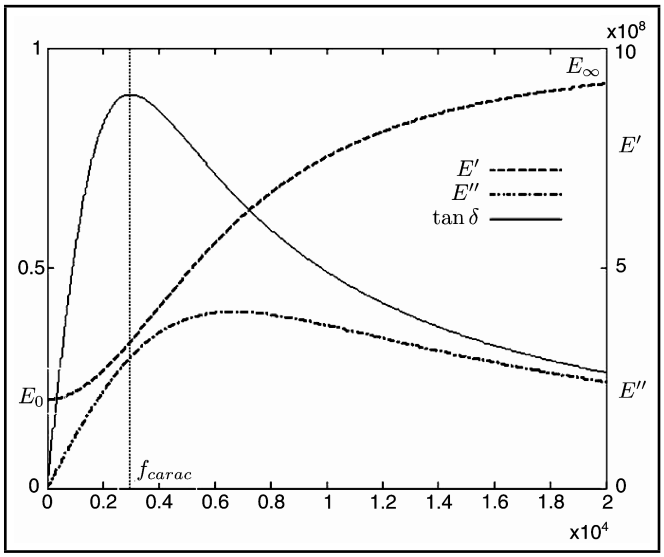

Figure 4. Example of a standard viscoelastic material.

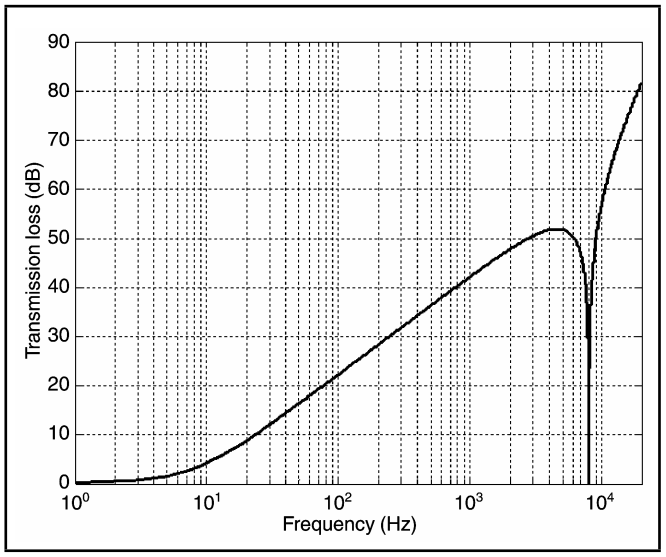

Figure 5. Response of a steel layer.

Table 1. Mechanical properties of a steel layer.

Thickness	3 mm
Young modulus	210 GPa
Poisson ratio	0.3
Density	7850 $\mathrm{Kg/m^3}$

Table 2. Comparison between model and Eq. (55).

Mechanical properties	$\rho = 7\,850\ \frac{\mathrm{Kg}}{\mathrm{m}^3}$, $E = 210\,\mathrm{MPa}$, $\nu = 0.3$		
Thickness	1.5 mm	3 mm	6 mm
Numerical frequency (TMM)	15 958 Hz	7 970 Hz	3 981 Hz
Theoretical frequency (Eq. 55)	15 673 Hz	7 836 Hz	3 918 Hz

This model is completely defined with three setting parameters, Fig. 4.

E_∞ : is the modulus in high frequency.
E_0 : is the modulus at low frequency.
f_{carac} : is the frequency when we have the maximum of damping.

Figure (4) shows the evolution of $\tan\delta$, E', and E'' over frequency. We note that at low and high frequencies, the viscoelastic material behaves as if it were elastic respectively with modulus E_0 and E_∞. We note also that at those two extremes, the damping coefficient $\tan\delta$ is very small. Whereas in between it passes through a maximum at the characteristic frequency.

4. NUMERICAL RESULTS

4.1. Acoustic Behavior of a Simple Layer

4.1.1. Typical response

The main characteristics of the tested layer are given in Table 1.

Figure (5) shows the response of a steel layer subjected to an incident wave at $\theta = \pi/4$. We note that the evolution of the transmission loss is characterized by three regions: (1) while $f < f_{coin}$, we have an increase of 6 dB/octave in this region the response is controlled by the mass of the plate; (2) around f_{coin}, we have a damping control, and (3) for $f > f_{coin}$, we have an increase of 18 dB/octave. The response is controlled by stiffness.

4.1.2. Coincidence frequency

When a structure is acoustically excited, the frequency at which the speed of the forced bending wave in the structure and the speed of the free bending wave are equal is called the coincidence frequency. At this frequency the capacity of isolation of the panel is very low.

When a sound wave, with a celerity c, strikes the panel at an angle of incidence θ, it produces in the plate a trace wave, called a forced wave. The speed of this forced bending wave is $c/\sin\theta$.

The speed of the free bending waves of a plate is[13]

$$c_b^4 = \frac{\omega^2 D}{\rho}; \tag{54}$$

where $D = \frac{E\mathrm{l}^3}{12}(1-\upsilon^2)$, is the flexural rigidity, and ρ is plate density.

Coincidence occurs when the speed of the forced bending wave matches the speed of the free bending wave $c_b = c/\sin\theta$; thus, we obtain

$$\omega_{coin}^2 = \frac{c^4\rho}{D\sin^4\theta}. \tag{55}$$

As a numerical validation, the coincidence frequency is obtained with TMM method then compared with theoretical results for the same configuration. Figure (5) shows the acoustic response of a plate and highlights the coincidence frequency due to an incident wave at $\theta = \pi/4$. This frequency is situated at 7 979 Hz, which agrees with theoretical results of 7 836 Hz. Table 2 regroups some other comparisons between numerical and theoretical frequencies computed with different thicknesses of studied plates. A good agreement is observed between the numerical and the theoretical results.

4.1.3. Diffuse field

In practice, sound waves are usually striking a partition from many angles simultaneously (Fig. (6)), (e.g., the wall of a room or a window exposed to traffic noise). The appropriate transmission coefficient can be calculated for a diffuse field with the

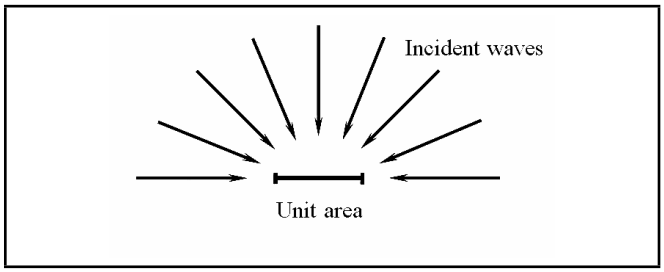

Figure 6. Diffuse field.

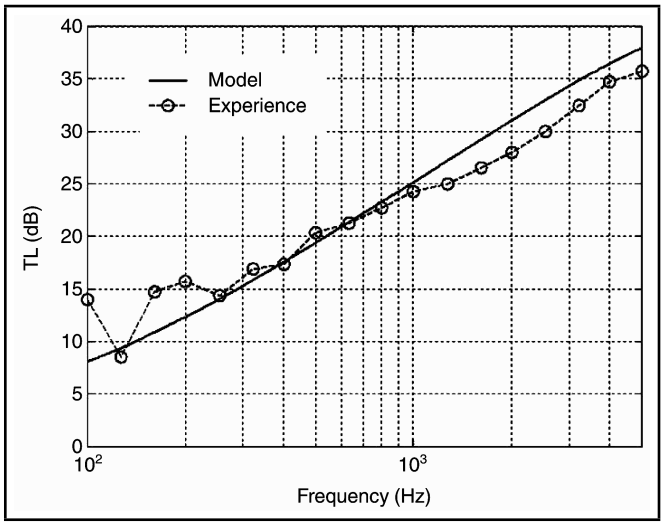

Figure 7. Comparison between model and experience.[15]

Table 3. Characteristics of the tested plate.[15]

Plate thickness	E	υ	ρ
1.1 mm	70 GPa	0.33	2 700 Kg/m^3

following expression:[9]

$$\mathrm{TL} = -10\log_{10}\int_0^{\theta_{max}} |T(\theta)|^2 \cos(\theta)\sin(\theta)\,\mathrm{d}\theta; \qquad (56)$$

with $\theta_{max} = 78°$, an angle proposed by Beranek.[14] This angle gives a good agreement between model and experience.

In order to validate the TMM approach in a diffuse field, we compare in Fig. (7) the experimental results issued from the literature to the numerical response obtained by the developed model.[15] The characteristics of the tested panel are presented in Table 3.

Figure (7) shows a good agreement between the model and the testing results. Therefore the model adequately describes the behavior of plates even though the model does not take into account the edge effect.

4.1.4. The mass law

Figure (8) shows the comparison of the acoustic response of three plates by increasing their mass by the double. According to Fahy,[16] doubling the mass of a panel, by doubling the thickness of the plate or using a material twice denser than the first, can improve insulation with 6 dB per octave. The previous comments are verified by the developed model.

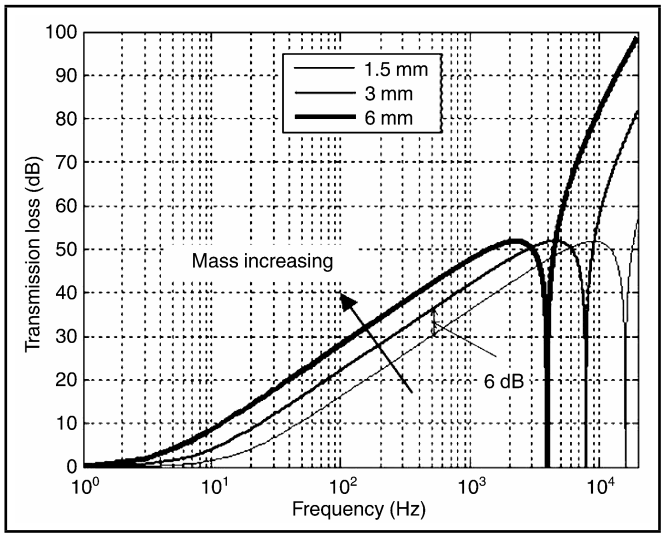

Figure 8. TL with increasing mass by double.

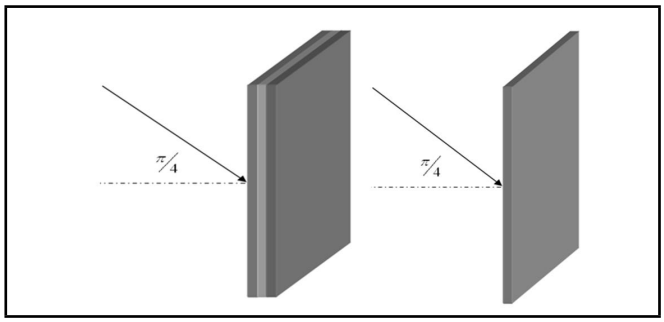

Figure 9. Response of panels with the same mass.

Table 4. Characteristics of the viscoelastic material.

E_0 (MPa)	E_∞ (MPa)	f_{carac} (Hz)
10	100	5 000

4.2. Study of Double-layer and Triple-layer

For all numerical results proposed in this section, the main characteristics of the studied viscoelastic materials are regrouped in Table 4.

In the first example, the acoustic response of a triple-layer panel with a viscoelastic core is compared to a simple steel layer having the same mass (Fig. (9)). The geometric and mechanical characteristics of the panel are regrouped in Table 5.

Figure (10) displays a comparison of the transmission loss factor against the frequency. The presented results show some disparities, although we have the same excitation and mass. In the first region, the same behavior is observed, and the response is governed by the mass law. It is also noted that due to the contribution of the viscoelastic layer, the coincidence frequency reaches the inaudible domain at a higher frequencies.

Table 5. Characteristic of the compared panels.

	Thikness (mm)	E (GPa)	υ	ρ $\left(\frac{\mathrm{kg}}{\mathrm{m}^3}\right)$
Layer 1 (steel)	2	210	0.3	7850
Layer 2 (viscoelastic)	5	$0.01 \rightarrow 0.1$	0.49	950
Layer 3 (steel)	2	210	0.3	7850
equivalent layer (steel)	4.6	210	0.3	7850

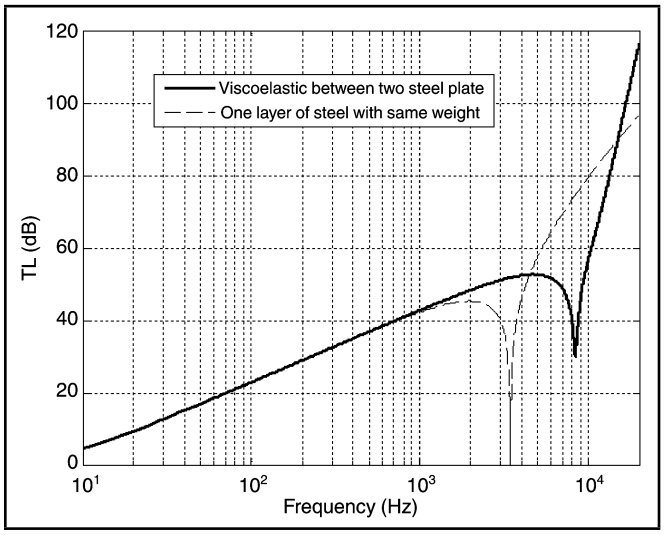

Figure 10. Comparison between triple-layer panel with viscoelastic core and simple layer panel.

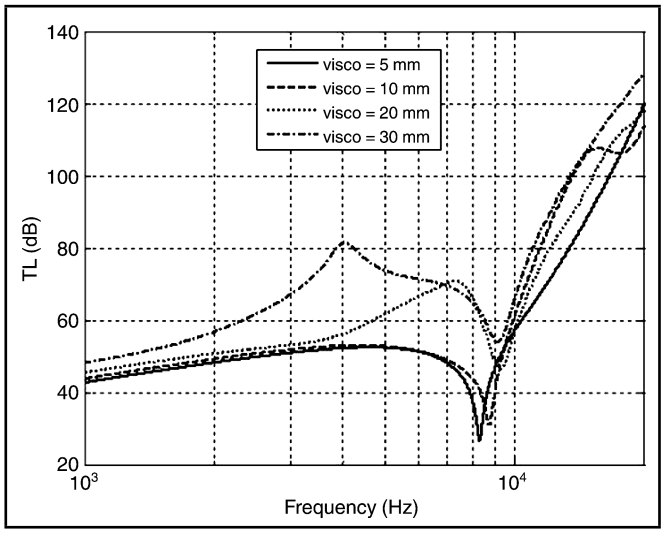

Figure 12. Effect of the viscoelastic layer.

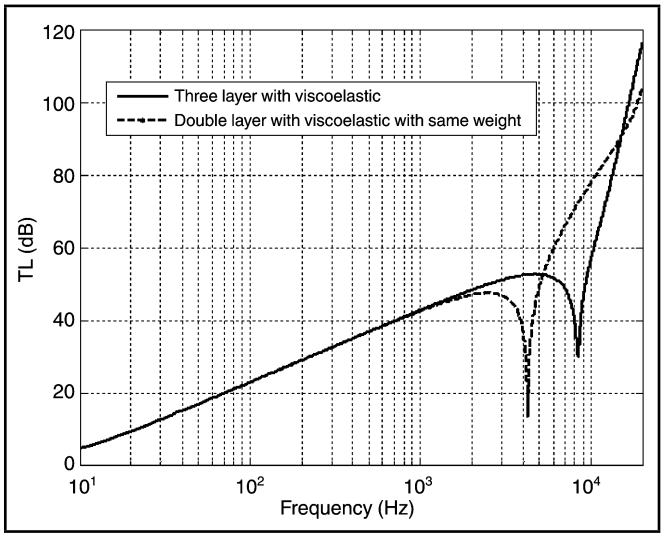

Figure 11. Response of triple-layer and double-layer with same mass.

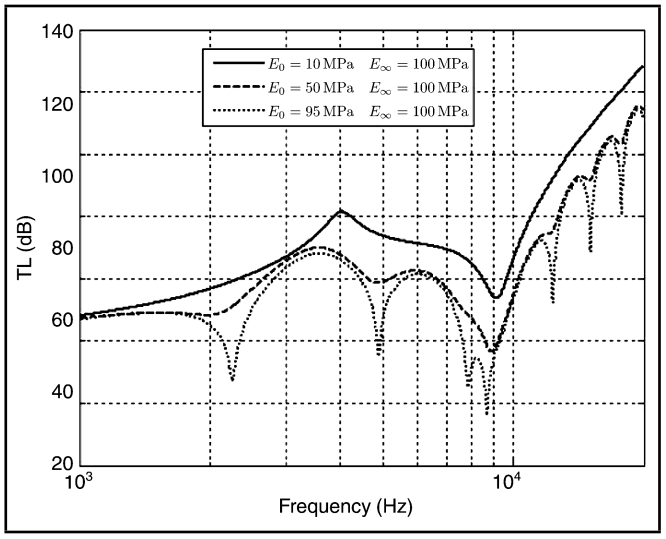

Figure 13. Influence of the damping effect.

In order to find the best arrangement of layers in terms of sound insulation, two configurations are studied. Figure 12 shows the comparison between a triple-layer panel (2 mm steel / 5 mm viscoelastic / 2 mm steel) and the two-layer panel (4 mm steel / 5 mm viscoelastic), which is equivalent in mass. It is clear that the first configuration is characterized by a higher coincidence frequency, and therefore a better acoustic insulation (Fig. (11)).

4.3. Parametric Study of the Viscoelastic Layer

In order to study the effect of the mechanical parameters of the viscoelastic material on the acoustic response different values of E_0, f_{carac}, and thickness are tested.

First, a viscoelastic layer with a thickness ranging from 5 mm to 40 mm is sandwiched between two layers of steel of 2 mm thick each.

Figure (12) shows the effect of increasing the thickness of the viscoelastic layer. We note that the insulation especially near the coincidence frequency is improved. The total transparency at this frequency is mitigated. Beyond this frequency, where the stiffness controls the response, we see a greater slope and, therefore, more insulation is obtained.

In the second investigation, the same configuration of a multilayer panel is adopted (2 mm steel / 40 mm viscoelastic / 2 mm steel), and the parametric study is focused on the viscoelastic Youngs modulus. Figure (13) shows the results due to the variation of the interval between E_0 and E_∞. It is noted that the acoustic insulation of the multilayer panel decreases by the reduction of the variation between E_0 and E_∞. In fact, the damping effect of the viscoelastic material is considerably reduced, which explains the TL evolution. In this case the behavior of the multilayer panel looks like a double wall because the Youngs modulus is almost constant.

Finally, The same multilayer panel is considered (2 mm steel / 40 mm viscoelastic / 2 mm steel), with $E_0 = 50\,\mathrm{MPa}$ and $E_\infty = 100\,\mathrm{MPa}$ being kept constant, while the characteristic frequency f_{carac} ranges from 1 000 Hz to 5 000 Hz. Figure (14) illustrates a comparison of TL evolution against frequency. The presented results show an improvement of the acoustic insulation by increasing f_{carac} of the viscoelastic layer. We note also that coincidence frequency of the multi-

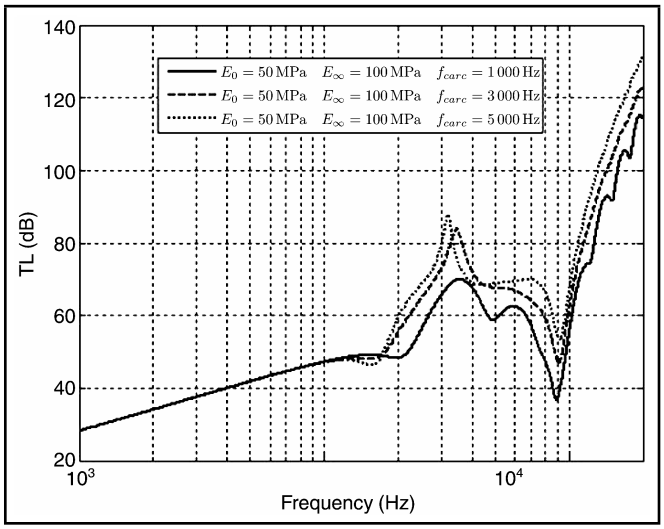

Figure 14. Influence of f_{carac}.

layer panel is insensible to the variation of the characteristic frequency of the viscoelastic material.

5. CONCLUSION

In this paper, a convenient method for predicting the acoustic behavior of a multilayer panel was developed. The well-known transfer matrix method was adopted for its simplicity of programming and timely execution. The method developed takes into account the behavior of the viscoelastic material in a configuration of multi-layered panels. Computational results were compared to experiments found in the literature. Numerical simulations were carried out to investigate the effects of different mechanical characteristics of the viscoelastic layer. Different layer arrangement was also tested in order to find the best configuration of a multilayer panel in terms of acoustic insulation. This method can be associated with an optimization program like GA algorithm and can take into account a layer of Biot materials.

REFERENCES

[1] Thomson, W. T. Transmission of elastic waves through a stratified solid medium, *Journal of Applied Physics*, **21**, 89–93, (1950).

[2] Snowdon, J. C. Mechanical four pole parameters and their applications. *Journal of Sound and Vibration*, **15**, 307–323, (1971).

[3] Folds, D. L. and Loggins, C. D. Transmission and reflection of ultrasonic waves in layered media. *Journal of the Acoustical Society of America*, **62**(5),1102–1109, (1977).

[4] Nayfeh, A. N. The general problem of elastic wave propagation in multilayered anisotropic media. *Journal of the Acoustical Society of America*, **89**(4), 1521–1531, (1991).

[5] Sastry, J. S. and Munjal M. L. A transfer matrix approach for evaluation of the response of a multi-layer infinite plate to a two-dimensional pressure excitation. *Journal of Sound and Vibration*, **182**(1), 109–128, (1995).

[6] Munjal, M. L. Response of a multi-layered infinite plate to an oblique plan wave by means of transfer matrices. *Journal of Sound and Vibration*, **162**(2), 333–343, (1993).

[7] Lee,C. M. and Xu, Y. A modified transfer matrix method for prediction of transmission loss of multilayer acoustic materials. *Journal of Sound and Vibration*, **326**, 290–301, (2009).

[8] Villot, M., Guigou, C. and Gagliardini L. Predicting the acoustical radiation of finite size multi-layered structures by applying spatial windowing on infinite structures. *Journal of Sound and Vibration*, **245**(3), 433–455, (2001).

[9] Allard, J. F., Lafarge, D., and Brouard, B. A general method of modelling sound propagation in layered media. *Journal of Sound and Vibration*, **183**(1), 129–142, (1995).

[10] Soula, M. and Chevalier, Y. The fractional derivative in rheology of polymers — application to the elastic and viscoelastic behavior of linear and nonlinear elastomers (La dérivée fractionnaire en rhéologie des Polymères - application aux comportements élastiques et viscoélastiques linéaires et non linéaires des lastomères. *ESAIM Proceeding*, **5**, 87–98, (1998).

[11] Cremer, L., Heckl, M., and Ungar, E. E. *Structure-Borne Sound*, Heidelberg, Springer-Verlag, (1988).

[12] François, D. Technical Engineering M 4 151-1. Mechanical behavior of metals. (Technique de lingénieur M 4 151-1. Lois de comportement des métaux) (2004).

[13] Renji, K. and Near, P. S. Critical and coincidence frequencies of flat panels. *Journal of Sound and Vibration*, **205**(1), 19–32, (1997).

[14] Beranek, L. L. The transmission and radiation of acoustic waves by solid structures, *Noise Reduction*, New York, McGraw-Hill, (1971).

[15] Pellicier, A. and Trompette, N. A review of analytical methods, based on the wave approach, to compute partitions transmission loss. *Applied Acoustics*, **68**, 1192–1212, (2007).

[16] Fahy, F. *Sound and structural vibration*, Great Britain, London, (2001).